GeoPlanning
Journal of Geomatics and Planning
Vol. 11, No. 1, 2024

e-ISSN: 2355-6544

Received: 31 October 2023;
Accepted: 13 February 2024;
Published: 08 March 2024.

Keywords:
LST, NDVI, NDBI, Remote Sensing

*Corresponding author(s)
email: pmaglipon@gmail.com

Original Research Open access

Tracking the Temporal Changes in Land Surface Temperature, Vegetation, and Built-up Patterns in Rizal Province, Philippines using Landsat Imagery

Pauline Angela Sobremonte-Maglipon[1,2*] Anne Olfato-Parojinog[1,2] King Joshua Almadrones-Reyes[3,4] James Eduard Limbo-Dizon[3,4] and Nikki Heherson A. Dagamac[1,2,3,4]

1. *Department of Biological Sciences, College of Science, University of Santo Tomas, España, Manila, 1008, Philippines*
2. *The Graduate School, University of Santo Tomas, España, Manila, 1008, Philippines*
3. *Research Center for the Natural and Applied Sciences University of Santo Tomas, España, Manila, 1008, Philippines*
4. *Advanced Educational Program, Thai Nguyen University of Agriculture and Forestry Quyết Thắng, Thái Nguyên, Vietnam*

DOI: 10.14710/geoplanning.11.1.71-84

Abstract

The Rizal Province was subjected to a series of natural and human-induced disturbances throughout the years. Currently, the area is undergoing urbanization which in turn results in shifts in the extent of impervious surfaces that can intensify heat-related health concerns, increase energy consumption for cooling, and alter local weather patterns. This study uses remote sensing images from to quantify the various environmental considerations that remain undocumented and unmapped for areas caused by changes in land use and land cover from Landsat Collection 1- Level 1 (Landsat 4-5 ™ C1- Level 1 & Landsat 8 OLI/ TIRS C1 Level 1) and calculated three parameters namely, (i) Land surface temperature (LST), (ii) Normalized Difference Vegetation Index (NDVI), and (iii) the Normalized Difference Built-up Index (NDBI). The results showed the following: (i) an increase in the vegetation cover from 1993-2020 showed a decrease in LST from 29.34°C to 24.03°C, (ii) the relationship between LST and NDBI is directly proportional, whereas an inversely proportional relationship can be observed between LST and NDVI, and (iii) there is a fluctuating LST due to the changes in the land cover of the study site for almost three decades. This implicates the extensive shift in the ambient temperature of Rizal which further emphasizes the effects of the modification in certain land use land cover classifications, especially in vegetation cover and urban development. This highlights how human-induced and natural factors significantly contribute to the release of heat and ambient temperature, thus, accentuating the need for sustainable urban planning.

1. Introduction

For the past several decades, urbanization in various megacities especially in developing countries such as the Philippines has been steadily expanding in response to the increase in human population. As a result of this, urban development continuously ensues to meet the living demands of the rapidly growing population (Doygun & Alphan, 2006; Ramachandra et al., 2015; Buchori et al., 2022). Unfortunately, the built up of urban areas has led to the increase in land surface temperature (LST) due to the accumulation of solar heat retention from infrastructural materials such as cement, asphalt, concrete, and steel, all of which are characterized to have high heat capacities (Stempihar et al., 2012; Uddin et al., 2022; Morris et al., 2017). In addition, other forms of human-induced heat emissions including fuel and biomass burning are contributing factors to the increase of LST

(Ekwurzel et al., 2017). This concept is otherwise known as the Urban Heat Island (UHI) effect. The observed warming in urban areas corresponds to the land-use changes, usually that from vegetation to settlements (Fang et al., 2011). The consequences of the UHI effect extend beyond mere temperature increases; it can significantly alter urban ecological systems and exert various ecological and environmental impacts on urban climates, hydrological situations, soil properties, atmospheric environments, biological habitats, material cycles, energy metabolism, and residents' health (Yang et al., 2016). These changes can render urban areas more vulnerable to economic and socio-political perturbations (Chase et al., 1999; Vitousek et al., 1997; Kasperson et al., 1995).

The pioneering observation of the UHI phenomenon initially introduced by Luke Howard in 1818 indicated the global acknowledgment of a substantial urban climatic and environmental predicament (Zhou & Chen, 2018). UHI, widely prevalent across urban landscapes, encompasses elevated heat capacity, thermal conductivity, and predominantly impervious surfaces, which amplify heat absorption and retention relative to rural locales (Gaur et al., 2018; Naikoo et al., 2022). Additionally, the proliferation of urban structures aggravates heat absorption by means of recurrent reflections and absorption, much as the presence of establishments and buildings reduce urban air circulation, further compounding heat accumulation (He et al., 2007; Zhou & Chen, 2018). Because of this, megacities confront steadily escalating UHI magnitudes, exacerbating discomfort in the urban thermal setting, especially during warmer seasons, thereby establishing prolonged reliance on air conditioning by inhabitants, hence, giving rise to an extended levels of anthropogenic heat discharge (Zhou et al. 2011; Zhou & Chen, 2018). Similar studies highlight mitigating UHI implications to diminish the adverse effects on urban inhabitants' health and well-being, advocating for a deeper understanding and definite interventions in urban development and design to foster a holistic approach towards sustainable and resilient urban planning.

An analysis that can evaluate the UHI effect is the LST analysis, which is considered to be one of the most vital domains in assessing the physical systematic series of surface energy (Chen et al., 2013). LST is the land surface's radiative skin temperature measured by means of a remote sensor. Additionally, it is approximated in distinction to geostationary satellites' top-of-atmosphere brightness temperatures taken from their infrared spectral channels. Information gathered by means of this analysis dispenses data regarding both temporal as well as spatial variations of the land (Chen et al., 2013). This concept is generally used in a wide range of fields spanning critical concepts in environmental science such as evapotranspiration, hydrological cycle, urban climate, climate change monitoring, vegetation records, and other related studies (Guha et al., 2017; Chen et al., 2013). The acquisition of LST through multi-temporal remote sensing may be further supported by indices such as (1) the Normalized Difference Vegetation Index (NDVI) and (2) the Normalized Difference Built-up Index (NDBI). Simply put, NDVI is used as an indicator for vegetation cover, whereas NDBI is for levels of urbanization. These are vital indices as they are used for correlation (Bala et al., 2018; Malik et al., 2019). The analysis of LST combined with NDVI and NDBI data can provide indications regarding the correlation among vegetation and build-up indices as well as surface temperature (Chen et al., 2013). Substantial alterations in terms of LULC are brought about by anthropogenic and natural factors impacting heat emission of LST (Malik et al., 2018). The results that may be collated in this component of the study can illustrate the extensive shift in the ambient temperature of Rizal, which can establish evidence of the implications of the changes in land use land cover (LULC) classifications in the area.

Several studies have been carried out in the Philippines that utilize remote sensing to investigate, as well as address issues regarding urbanization and its effects. For instance, are the two recent studies that have been conducted in Metropolitan Manila. Limbo-Dizon and Dagamac (2023) detect how the coastline of Manila was affected by the rapid urban development over the past decades. Almadrones-Reyes and Dagamac (2022) assessed LULC and LST changes in Metropolitan Manila using Landsat imagery. Similarly, Tiangco et al. (2008), investigated the LST of Metro Manila, nonetheless, Advanced Spaceborne Thermal Emission and Reflection Radiometer (ASTER) was used. On the other hand, Tinoy et al. (2019), generated spatiotemporal hot and cold spot occurrence maps by utilizing LST images in Davao City. While numerous studies have explored urbanization and its impacts in the Philippines, focusing primarily on metropolitan areas like Manila, and Davao,

research in semi-urban regions such as the Province of Rizal remains limited (Limbo-Dizon & Dagamac, 2023; Almadrones-Reyes & Dagamac, 2022; Tiangco et al., 2008; Tinoy et al., 2019). This particularly serves a significant purpose as semi-urban areas are known to be transitional zones between natural and human-modified landscapes (Meeus & Gulinck, 2008). With that, this study aims (i) to generate an LST map in Rizal from the years 1993, 1997, 2014 and 2020; (ii) to calculate the NDVI and NDBI values of the said years; and (iii) to determine and interpret the relationship of LST to NDVI and NDBI in the study area. Investigating abiotic dynamics in areas that have yet to be studied can potentially provide novel insights, in a regional aspect, into the processes driving socio-economic change and environmental impact, which, in turn, can contribute to sustainable development strategies. With these set objectives, research gaps may be bridged by elucidating the understanding of biological processes, particularly regarding abiotic factors such as vegetation and temperature.

2. Data and Methods

2.1. Study Area

Rizal (see Figure 1), a rapidly growing province situated in Region IV-A within the northern-central region of CALABARZON in Luzon, is recognized as one of the Philippines' distinguished first-class provinces. It is specifically located west of Metro Manila and borders Bulacan to the north, Quezon to the east, and Laguna to the southeast. Notably, it stretches along the northern banks of Laguna de Bay, the largest lake in the Philippines. Characterized by a rugged terrain, Rizal Province is nestled within the western slopes of the southern section of the Sierra Madre Mountain range and spans a total area of 1,182.65 square kilometers. The latitudinal and longitudinal extent of Rizal are delineated by these coordinates: 14°28'69.79"N-14°89'24.46"N and 121°09'51.58"E-121°46'65.31"E.

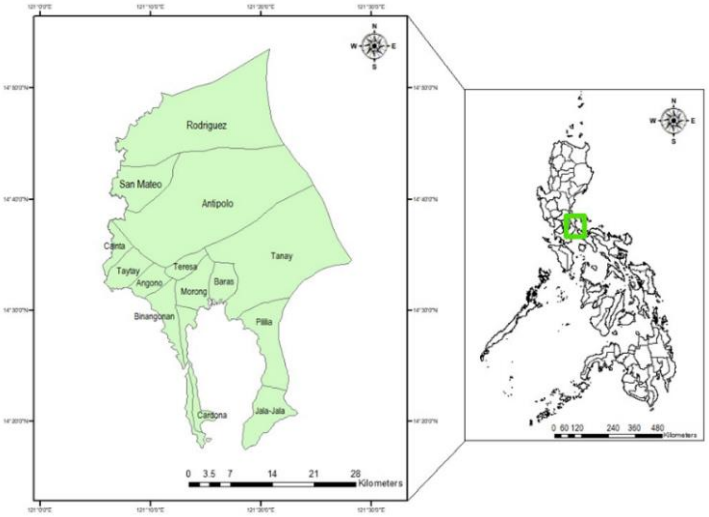

Figure 1. Map of the study area, Rizal, Philippines.

The province consists of 1 city and 13 municipalities, with 8 of these municipalities classified as first-class, including Angono, Binangonan, Cainta, Pililla, Rodriguez, San Mateo, Tanay, and Taytay. In contrast, there are 2 second-class municipalities, Morong and Teresa, while Cardona and Baras represent the third and fourth class categories, respectively. This demarcation encompasses a total of 189 barangays, collectively shaping the province's administrative boundaries. Serving as capital city of Rizal, Antipolo plays a pivotal role in anchoring this vibrant province. As per the 2020 census data from the National Statistics Office of the Philippines, Rizal Province is now home to a substantial population, ranking as the fourth most populous province in the country. Over the course of 117 years, it has experienced a remarkable demographic transformation, with its population burgeoning from 50,095 residents in 1903 to a significant 3,330,143 individuals by 2020. This remarkable growth signifies an increase of 3,280,048 people, reflecting an expansion rate of 3.07%. Notably, this surge translates to an additional 445,916 individuals compared to the 2015 population count of 2,884,227.

Classified under the Koppen climate system as Type 1, the study area features two distinct seasons: a dry season spanning November to April and a wet season from May to October. This climate type is conducive to both industrial and agricultural development. Moreover, its strategic location makes Rizal an attractive prospect for business ventures and settlements, including the establishment of ecotourism destinations, thereby drawing potential investments to the region. Additionally, its proximity to Metropolitan Manila renders it susceptible to the effects of rapid urbanization, given its suitability for urban development.

2.2. Data Acquisition

As a means to detect changes in LST in the study area, remotely sensed imageries obtained from the Landsat Collection 1-Level 1 (specifically, Landsat 4-5 ™ C1-Level 1 and Landsat 8 OLI/TIRS C1 Level 1) accessible via the USGS EarthExplorer were used. This resource offers an extensive catalog of satellite and aerial images that are readily accessible for comprehensive data analysis. The process of satellite imagery selection took into account several critical criteria to ensure maximum accuracy and reliability. These criteria encompassed the necessity for minimal Land and Scene Cloud cover, both of which were stipulated to be below 10%, as well as the requirement that the imagery be captured during daylight hours.

Table 1. Details of Landsat 5 ™ C1- Level 1 and 8 OLI / TIRS C1 Level Imagery Utilized for Classification.

Satellite	Sensor	Acquisition date	Landsat Product Identifier	Source
Landsat 5	Multispectral Scanner and the Thematic Mapper	05-04-1993	LT05_L1TP_116050_19930504_20170119_01_T1	https://earthexplorer.usgs.gov/
Landsat 5	Multispectral Scanner and the Thematic Mapper	10-22-1997	LT05_L1TP_116050_19971022_20161229_01_T1	https://earthexplorer.usgs.gov/
Landsat 8	Operational Land Imager and Thermal Infrared Sensor	02-07-2014	LC08_L1TP_116050_20140207_20170426_01_T1	https://earthexplorer.usgs.gov/
Landsat 8	Operational Land Imager and Thermal Infrared Sensor	12-24-2020	LC08_L1TP_116050_20201224_20210310_01_T1	https://earthexplorer.usgs.gov/

Over a period spanning 27 years (1993, 1997, 2014, and 2020), a total of four remotely sensed images were procured (see Table 1). These specific years were chosen due to their alignment with the additional criteria established for quality assurance. Furthermore, to demarcate the boundaries of Rizal province within the remotely sensed imagery, an Administrative Boundary dataset from the DIVA-GIS database was layered and clipped. This comprehensive approach allowed satellite imageries that met stringent quality standards to be obtained, facilitating an accurate and reliable analysis of the study area's LST. The schematic diagram summarizing the major steps in data acquisition and processing is seen in Figure 2.

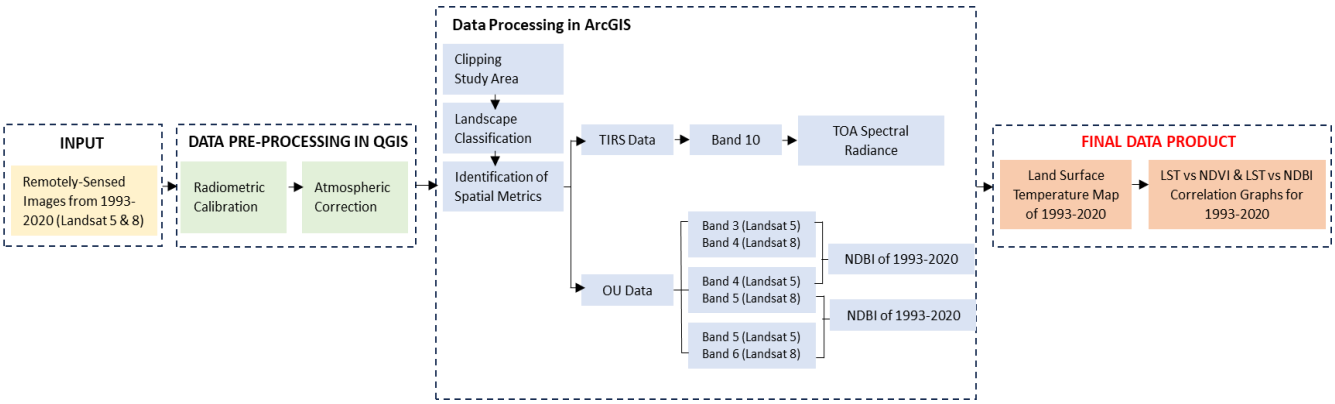

Figure 2. Methodological Framework for Assessing the Land Surface Temperature in Rizal

2.3. Data Processing

Prior to LST analyses of the remotely sensed data acquired, the images had also undergone image preprocessing through QGIS 3.20 Odense. Atmospheric correction was employed since it is important to minimize the differences in surface reflectance (SR), which will enable to conduct a direct comparison between

variations of image dates and different sensors (Nazeer et al., 2014). The Semi-automatic Classification Plugin was utilized, wherein Landsat data to Top of the Atmosphere (TOA) reflectance and brightness temperature, with DOS1 Atmospheric correction. Prior to the Supervised Classification of the LULC categories, an adjustment in brightness and contrast of the remotely sensed images is made through ArcGIS for more accurate classification. In addition, the area of the Rizal province was delineated with the use of the Administrative Boundary shapefile acquired through the DIVA-GIS database and extracted by mask through ArcGIS geoprocessing tools.

2.4. Land Surface Temperature Analysis

Considering that the data acquired from 1993-2014 are from Landsat 5 TM and data from 2020 is from Landsat 8 OLI, the description, wavelength, and resolution of each Landsat corresponds to the different designation of band number, hence, varying equations were used to retrieve certain variables, values of both indices, and the LST of each respective year. This may be due to the complexity that Landsat 8 brings, seeing that it is the first of its kind, it has Thermal Infrared Sensors (TIRS) as well as an Operational Land Imager (OLI) incorporating spectral bands of 1 to 11 with bands of 10 and 11 being the thermal bands. On the other hand, Landsat 5 uses a Landsat Thematic Mapper (TM) sensor, and out of its 7 spectral bands, band 6 was used for the conversion of spectral radiance so as to acquire the LST (Poursanidis et al., 2015).

2.5. Retrieval of Land Surface Temperature Calculation from Landsat 5

Retrieval of LST initiated with obtaining the Digital Number (DN) image from band 6. The DN was converted to top-of-atmosphere (TOA) radiance also known as the spectral radiance, which is denoted by the symbol L_{λ}., L_{min}, and $Lm_{ax\lambda}$ (which is obtained from the following calculation Equation 1) represent the detected scaled spectral radiance to the minimum and maximum quantized calibrated pixel value, denoted by $QCAL$, in digitized numbers, both of these spectral radiances are in W/(m² ster m) (Barsi et al., 2003; Qin et al., 2001).

$$L\lambda = \frac{(L_{max\lambda} - L_{min\lambda})}{(QCALMAX - QCALMIN)(QCAL - QCALMIN)} + L_{min\lambda} \ldots\ldots (Eq.1)$$

Spectral radiance is, then, converted into temperature in Kelvin. This is denoted by T which represents the effective at-satellite brightness temperature of TM6 in the calibration constants 1 and 2, which are represented by the symbols $K1$ and $K2$. The calibration constant values for Landsat 5 TM are as follows: $K1$ = 60.776 and $K2$ = 1260.56 (Schneider & Mauser, 1996). Once T is obtained, considering that the unit of temperature is Kelvin, it must be converted into degree Celsius by subtracting 273.15 (Equation 2):

$$T = \frac{K_2}{In\left(\frac{K_1}{L_T}\right)+1} - 273.15 \ldots\ldots\ldots\ldots\ldots\ldots\ldots (Eq.2)$$

2.6. Retrieval of Land Surface Temperature Calculation from Landsat 8

Similar to that of Landsat 5 TM, the initial step is to input a band, however, for Landsat 8 OLI the band number inserted into the application is band 10 for thermal infrared 1. The Equation 3, below represents the first conversion formula for Landsat 8 to obtain the top of atmospheric spectral radiance.

$$L\lambda = ML * Qcal + AL - Oi \qquad \ldots\ldots\ldots\ldots\ldots\ldots (Eq.3)$$

The radiance multiplicative band number is denoted by ML. It is then multiplied to the pixel values or the DN of the quantized and calibrated standard product. AL, on the other hand, is the additive rescaling factor that is distinct for each band. Lastly, Oi is the correction value for band 10 which is 0.29. Once spectral radiance was converted into reflection, the step that followed was the conversion of atmosphere brightness temperature (BT) by the use of the equation below, which utilized the same thermal constants, only with varying values due to the difference in band number used (Equation 4). The calibration constant values for Landsat 8 OLI band 10 are as follows: $K1$ = 774.89 mW and $K2$ = 1321.08 (Guha et al., 2017).

$$BT = \frac{K_2}{In\left(\frac{K_1}{L\lambda}\right)+1} - 273.15 \ldots\ldots\ldots\ldots\ldots\ldots (Eq.4)$$

The two indices utilized in the study were the NDVI and NDBI, both of which are derived from three reflectance bands, namely: visible, Near Infra-Red, and Short-Wave Infra-Red. In order to acquire the respective values of each index, computations were made possible by using the equation seen in Table 2.

Table 2. Retrieval of Indices Values

Index	Equation	Bands used in Landsat 5	Bands used in Landsat 8
Normalized Difference Vegetation Index (NDVI)	NIR – RED	Band 4 – Band 3	Band 5 – Band 4
	NIR + RED	Band 4 + Band 3	Band 5 + Band 4
Normalized Difference Built- up Index (NDBI)	NIR – RED	Band 5 – Band 4	Band 6 – Band 5
	NIR + RED	Band 5 + Band 4	Band 6 + Band 5

It is of utmost importance to retrieve the two indices as it is the required values used to calculate the proportion of vegetation. A method in quantifying the vegetation proportion from Wang et al. (2015), suggests that soil and vegetation NDVI values be included so as to fit to a more global context. However, considering the varying NDVI values of different geographical regions, in the case of the study it was best to simply use the minimum and maximum values of DN out of the NDVI image seeing that, generally, the NDVI value itself was quantified from the reflectivity of the spectral radiance (Avdan & Jovanovska, 2016).

$$P_v = \left(\frac{NDVI - NDVI_{min}}{NDVI_{max} - NDVI_{max}}\right)^2 \ldots\ldots\ldots\ldots\ldots\ldots (Eq.5)$$

Another aspect required to obtain an estimation of the LST is the land surface emissivity as it is used to indicate the emitted radiance (Jimenez-Munoz et al., 2006). The equation for the land surface emissivity is denoted by ε (Equation 6). The value 0.004 presented is considered the surface roughness constant (Sobrino & Raissouni, 2000). On the other hand, since the obtained NDVI denotes that the majority of the land surface is covered by soil, therefore giving an NDVI value of 0 to 0.2, an emissivity value of 0.986 is designated in the equation (Avdan & Jovanovska, 2016; Sobrino et al., 2004; Guha et al., 2017).

$$\varepsilon = 0.004 * P_v + 0.986 \ldots\ldots\ldots\ldots\ldots\ldots (Eq.6)$$

The determination of LST, in Celsius, is conditionally quantified by using the equation below; Equation 7 (Stathopoulou & Cartalis, 2007). The symbol ρ represents the wavelength of the emitted radiance, which is given an assigned value of 10.8 for band 10 in Landsat 8.

$$Ts = \frac{BT}{\left\{1+\left[\frac{\lambda BT}{\rho}\right]\text{In}\varepsilon\right\}} \ldots\ldots\ldots\ldots\ldots\ldots (Eq.7)$$

3. Results and Discussion

Four spatial distribution maps of the LST in Rizal were generated from ArcGIS. The various thermal signatures indicated in each of the LST maps are results of the presence of different land cover classes constituting distinct thermal properties. Fluctuations of temperature for these years are apparent. However, one aspect is shared among the retrieved data: relatively high temperatures are mostly centralized in the municipalities neighboring Metro Manila, where bare land, settlements, and population density are at their highest, causing higher concentrations of surface temperature. The spatial distribution of LST across the province of Rizal reveals that cities located in the Northern, Eastern, and Southern parts experience comparatively lower temperatures, whereas cities specifically in the Western section of the region have higher temperatures. The descriptive statistic exhibiting the values of LST, NDVI, and NDBI is presented in Table 3. These values, obtained from Landsat 5 TM and Landsat 8 OLI and TIRS satellites, range between 15.18°C and 40.31°C across the entire dataset. Based on 1200 points selected from the calibrated satellite imagery, the average LST for 1993, 1997, 2014, and 2020 is 29.34°C, 23.91°C, 25.59°C, and 24.03°C, respectively.

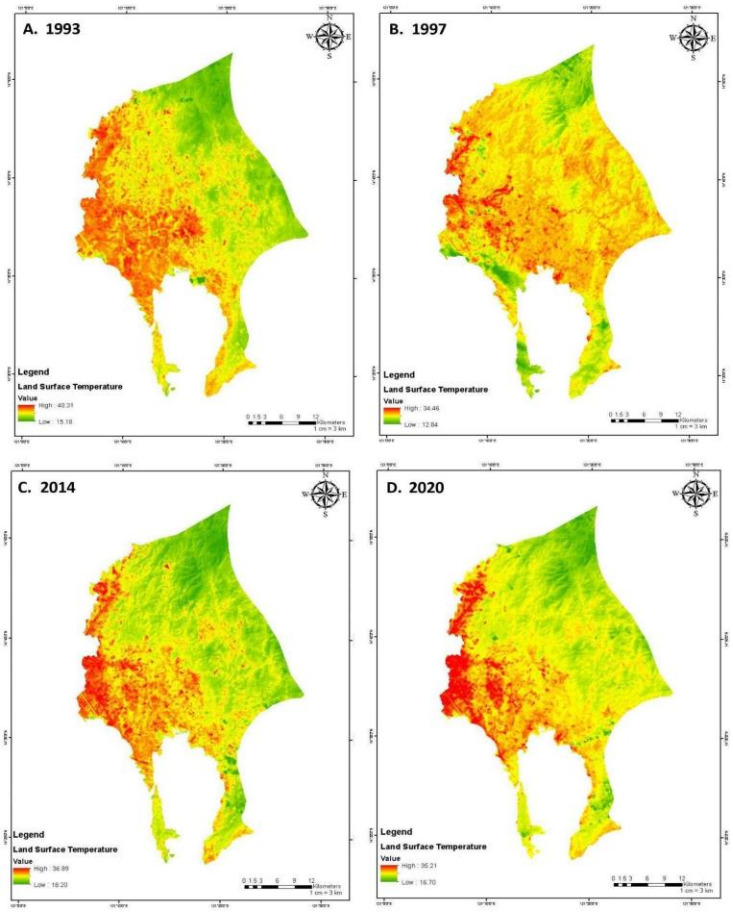

Figure 3. Land Surface Temperature Maps of (a) 1993, (b) 1997, (c) 2014, (d) 2020.

As shown in Figure 3a, the year with the highest surface temperature is 1993. This may be attributed to several biological phenomena that have taken place in Rizal during that particular year. Alongside this, it can also be observed that the Pearson r value for buildup was at its highest. By 1997, the LST visibly decreased in response to the significant decline of barren lands and settlements. This is succeeded by a significant rise in LST for the year 2014. However, in the most recent LST map, the data exhibits yet another decline in surface temperature values. Furthermore, it is from this year that the Pearson r value for buildup was second to the lowest, followed by the Pearson r value of 1997. Though almost having the same average LST values from 2014, the Pearson r value for NDBI decreased by 0.179. In comparison, the Pearson r value for NDVI has increased by 0.186. The results obtained are not limited to this alone. Correlations among LST, NDVI, and NDBI were additionally graphed (see Fig. 4 and Fig. 5). Based on the normalized difference indices, it can be observed that a decrease in vegetation and an increase in buildups lead to a rise in surface temperature. The end-to-end results showed an overall increase in the vegetation cover from 1993-2020 in correlation with the decrease in LST simulated in the study. These observations are in coherence with similar studies (Kumar et al., 2012; Zhou et al., 2014; Khandelwal et al., 2017; Tran et al., 2017; Peng et al., 2020; Saha et al., 2021).

3.1. NDVI vs LST Relationship

The NDVI is the quantification of the amount and vigor of vegetation present at the land surface. This index is related to vegetation to the utmost degree seeing that it can immensely reflect the near-infrared portion of the spectrum (Kumar et al., 2012). NDVI is susceptible to seasonal changes; therefore, its marginal variations can easily affect and modify the LST of an area. The relationship between LST and NDVI was determined to be inversely proportional through correlation analysis. In line with this, graphs were generated to further indicate the association between the two. As exhibited in Figure 4, LST increases as NDVI value decreases. This can be

supported by the negative Pearson correlation values of -0.754, -0.181, -0.568, and -0.353 for the 1993-2020 datasets, thus, this evidently designates how LST is negatively correlated with NDVI, further reinforcing the statement that areas with the highest amount of vegetation tend to have lower surface temperatures.

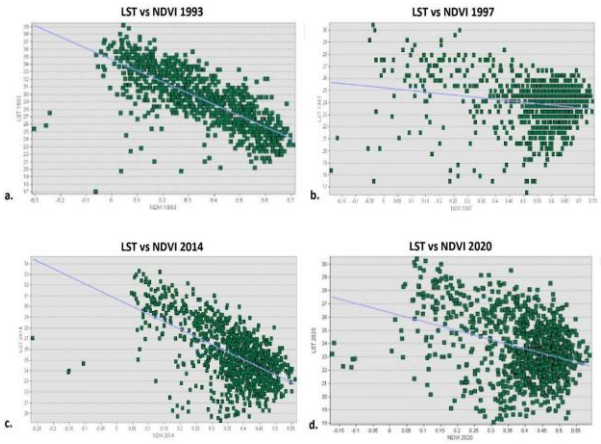

Figure 4. LST vs NDVI 2020 Correlation Graph of (a) 1993, (b) 1997, (c) 2014, (d) 2020

3.2. NDBI vs LST Relationship

One of the most established indices used in the processing and quantifying satellite data, especially that of monitoring the presence of build-up or settlements in each area, is NDBI (Kumar et al., 2012). The pixel values of NDBI range between negative (-) 1 to positive (+) 1, with greater values indicating highly concentrated build-ups. In this study, the relationship between NDBI and LST was assessed using the same methods for NDVI. However, in this analysis, the values of the Pearson correlation coefficient were all positive values, indicating that there is a strong and directly proportional correlation between the two variables, which corroborates the premise that as build-up increases, so does the surface temperature (Fig. 5).

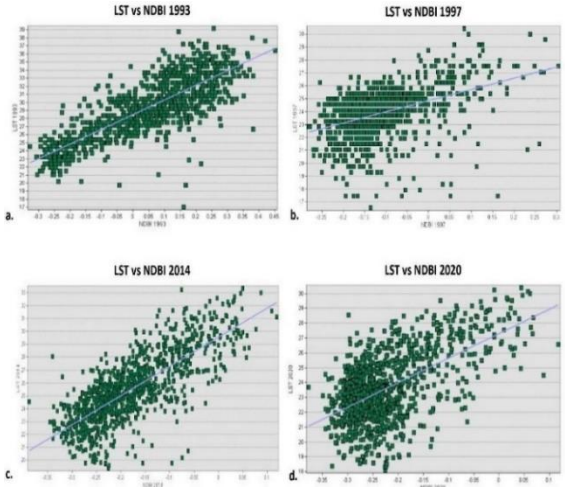

Figure 5. LST vs NDBI 2020 Correlation Graph of (a) 1993, (b) 1997, (c) 2014, (d) 2020

This statement is further reaffirmed, as the acquired results indicate that the highest LST values are found within built-up areas. From this, it can be deduced that densely urbanized areas generate higher surface temperatures. Hence, it is considered to be a primary factor in UHI, as previously confirmed by similar studies such as that of Malik et al. (2019) and Almadrones-Reyes & Dagamac (2022). The Pearson r value for the years 1993, 1997, 2014, and 2020 are as follows: 0.799, 0.428, 0.757, and 0.571. Though there may be visible fluctuations in these values, it overall indicates that there is a decline in buildup throughout the years.

There are numerous environmental parameters that heavily affect the modification and the transition of landscapes, and one such parameter is temperature. It is considered one of the major drivers of the productivity of vegetation in an area, which is directly interconnected with the concepts underlying NDVI and NDBI. In the case of this study, LST is strongly influenced by several factors such as solar incident radiation, angle of incidence of solar radiation, air temperature, and the expanse of vegetation; not to mention topography which encompasses several terrain conditions namely elevation, slope, and aspect. These are all linked to land surface properties like soil moisture and surface roughness (Khandelwal et al., 2017; Peng et al., 2020).

Table 3. Descriptive Statistics of LST, NDVI, and NDBI

LST				
Year	**Minimum**	**Maximum**	**Mean**	**SD**
1993	15.1795	40.3119	29.3395	3.7753
1997	12.8362	34.4621	23.9105	1.8889
2014	18.1954	36.8866	25.5940	2.7182
2020	16.7025	35.2090	24.0299	2.6917

Table 4. Descriptive Statistics of NDVI

NDVI					
Year	**Minimum**	**Maximum**	**Mean**	**SD**	**Pearson R**
1993	-0.3953	0.7333	0.3565	0.1876	-0.7539
1997	-0.3704	0.7692	0.5488	0.1569	-0.1815
2014	-0.1874	0.5895	0.3616	0.1143	-0.5677
2020	-0.1937	0.6072	0.3914	0.1228	-0.3527

Table 5. Descriptive Statistics of NDBI

NDBI					
Year	**Minimum**	**Maximum**	**Mean**	**SD**	**Pearson R**
1993	-0.4074	0.4958	0.0456	0.1650	0.7981
1997	-0.4203	0.3797	-0.1097	0.0953	0.4284
2014	-0.4188	0.1826	-0.1762	0.0920	0.7567
2020	-0.3982	0.2038	-0.2195	0.0844	0.5710

It can be regarded that areas with relatively high settlements and patches of barren lands have garnered higher LST values. This assertion aligns with the results produced by this study (see Fig. 3). This may be attributed to the lack of moisture from the soil surface in view of the natural disturbances that took place prior to 1993, such as a series of El Niño events between the years of 1986-1992, which induced severe stress on water resources (Hilario et al., 2009). Another aspect that highlights the increase in surface temperature is the high amount of solar radiation received in the region. It is also worth noting that during the same period as the natural disturbances, the urban core areas of Rizal, which are San Mateo, Cainta, Taytay, Angono, and Binangonan, have significantly contributed to the intensification of the UHI effect by means of increasing the distribution of hotspots through the establishments of several medium scale residential areas, including subdivisions (Regmi, 2017). In these highly concretized areas, NDVI values are at their lowest. The incremental consumption of energy, increase in built-up surfaces of concrete, asphalt, and the like, as well as a significant decline in both vegetation and water surfaces, all constitute the increase in LST (Kumar et al., 2012), as it is very much susceptible to various heat discharges coming from increased surface coverage of urban development.

This is in alignment with the research conducted by Olfato-Parojinog et al., which primarily focused on tracing the trends on the land use and land cover (LULC) in the province of Rizal. Their work that sheds light on the pattern of changes in LULC, and this study, set in the same study area and utilized data collected during the same years that ensures a directly comparable temporal and spatial context, corroborate each other's findings, providing robust evidence for LULC-LST dynamics. Just as Olfato-Parojinog et al. highlighted the LULC

changes, our findings also emphasize the importance of LST as a key indicator of the various modifications in LULC classes through time. The consistent patterns observed between this study and the work of Olfato-Parojinog et al.46 affirm the broader relevance of LULC-induced effects on thermal regimes, it becomes evident that the changes in LULC is directly correlated with changes in LST consistently exhibited similar trends.

Extreme lack of precipitation, coming in the form of insufficiency of rainfall as well as protracted drought, gives off direct and indirect effects not only on the ecological system but also to humans. The El Niño events that occurred in the years 2010 and 2014 have caused both meteorological as well as agricultural droughts. Meteorological droughts entail a deficiency in precipitation that lasts for a few months or so. Alterations in the pattern of atmospheric circulation bring about this phenomenon, which is primarily prompted by occurrences such as El Niño-Southern Oscillation (ENSO) causing anomalous modification in sea surface temperature. On the other hand, agricultural drought is centered on deficiencies pertaining to soil water, therefore, resulting in low soil moisture and higher LST. These two droughts have significantly contributed to reduced growth of vegetation and decline of crop productivity, further aggravating reduced humidity, not to mention higher rates of soil evaporation- resulting in drier environments.

Fortunately, even though major cities in the Philippines, especially those found in Metro Manila, have undergone notable increase in LST may it be due to natural disturbances like drought or anthropogenic activities such as urban expansion (Tiangco et al., 2008; Almadrones-Reyes & Dagamac, 2022), effective measures were put in place to address the situation in Rizal. The rejuvenation of vegetated areas may be attributed to the Laguna Lake Development Authority-Tanay Streambank Rehabilitation Project which is one of the reforestation campaigns conducted in Rizal from 2004-2014 that aimed to reforest 70 hectares of private land and establish 25 hectares of agroforestry land to increase riparian forest cover (Lasco et al., 2005). In line with this, the microwatershed occupying a notable portion of Tanay and the flank of the Sierra Madre Mountain Range located east of Rodriguez are prominent features found in the Northern and Eastern municipalities of Rizal that also substantially induced a cooling effect due to the presence of dense vegetation as measured by the vegetation index (Murdiyarso & Skutsch, 2006). The increase in the amount of vegetation due to the enrichment of soil moisture demarcates LST through the continuous change of latent heat coming from the surface transferred through the atmosphere by way of evapotranspiration. Furthermore, the decrease in patches of bare lands partakes in narrowing the discrepancies in radiant surface temperature (Sun et al., 2020). Both aforementioned statements give way to changes in the thermal responses and consequentially generate higher NDVI and lower NDBI values (Yuan & Bauer, 2007).

The reforestation program implemented has further improved the state of Rizal, in terms of its LST, as it has slowed down the rate of both agricultural and urban extensification, to a degree. Moreover, it has also increased the forest cover, which lowered the study area's Albedo, and, in turn, portions of its absorbed solar radiation increased at the surface. Because of this, shortwave radiation, especially during the daytime, is absorbed more, eliciting a warming effect. Nevertheless, this is counteracted by a higher amount of latent heat loss by means of increased evapotranspiration, which is primarily influenced by vegetation activity and soil moisture status (Peng et al. 2014). The positive modifications in the geophysical characteristics of Rizal have somehow rectified the previous predicaments from which the region had previously suffered. Evidently, by implementing effective and sustainable reforestation initiatives, it is feasible to progressively attain cooler temperatures. In essence, through integrating well-planned and environmentally responsible measures to restore forested areas, mitigating the effects of UHI, and contributing to the reduction of surface temperature is within the realm of possibility even for third-world countries, like the Philippines.

As the challenges of urban growth become more concerning throughout time, the significance of managing land resources is more pronounced in order to achieve sustainable development (UN, 2015; UNFCC, 2015; UN HABITAT, 2018). Thus, maximizing the available land resource through sustainable urban planning can achieve short- and long-term objectives given the prevailing land quality and socioeconomic factors in the locality (Verheye, 1997; Gebre et al., 2021). As the landscape has limited area for greeneries, giving priority for residential and industrial land use, the implementation of compact greenfields can minimize the effects of urban

heat islands. This can be in the form of establishment of street trees, forest parks, gardens, green walls and roofs, and green corridors and networks (Phelan et al., 2018; Maruna et al., 2019). Residential lands are the most spatially extensive in the peri-urban province, giving limitations for opportunities for vegetation establishment, thus, the government efforts towards urban greening must employ more strengthened and clear land use regulations, for the potential and existing tree covers even in private properties. In addition, involving the community and addressing their inputs and engagement is vital for strategizing policies and development, instilling responsibilities not just for the government, but also for the stakeholders (Phelan et al., 2018). Since peri-urban vegetation, such as in the case of the province of Rizal, plays a significant role in adaptation to climate change effect mitigation, looking further into the accurate and spatially explicit information on land suitability must be employed, involving stabilization of soils, reduction of pollutants, and overall environmental restoration (LaGro Jr., 2005; UN, 2015).

The findings from this study highlight the pressing necessity for a more sustainable and holistic environmental management strategy within the Rizal Province. As urbanization accelerates, temperature fluctuations are magnified, this supports previous studies related to the topic at hand (Yang et al., 2016; Yuan et al., 2007; Zhou et al., 2014). The documented increase in vegetation, coupled with a concurrent decrease LST, suggests a potentially ameliorating effect on heat islands. However, the direct relationship between LST and the NDBI points to the potential worsening of urban heat islands, posing serious challenges to local climate resilience and human well-being, if left unchecked. Furthermore, the inverse relationship between LST and the NDVI accentuate the ecological implications of urban expansion on vegetation. These shed light on the intricate dynamics of land use change, temperature regulation, and ecosystem health within Rizal Province.

4. Conclusion

This study sheds light on the dynamic interplay between land cover classes and LST in the Rizal Province. Over the years, the region has undergone modifications brought about by natural and anthropogenic-driven disturbances that added to the complexity of its already unique landscape. By correlating LST to NDVI and NDBI, significant insights have emerged. The observed increase in vegetation cover from 1993 to 2020 has corresponded to a notable decrease in LST, pointing out the cooling effect of increased green spaces. Additionally, this highlights the role of land cover in influencing temperature patterns. The study's documentation of fluctuating LST, attributed to nearly three decades of shifts in vegetation and built-up areas, accentuate the profound impact of both anthropogenic and natural factors on heat emissions and ambient temperature. These findings emphasize the continuous need for strict adherence of evidence-based land use and environmental policies to ensure a sustainable development towards urbanization and facilitate a harmonious coexistence with the environment in the Rizal Province, where the intricate relationship among various land cover classifications play a pivotal role in the LST of the area.

Given the significant role in assessing land cover and its influence on LST, future research should delve into the socio-economic drivers of the changes in the landscape and integration of the flows of urbanization in the province to address the mechanisms of urban expansion. This can be in the form of integration of socio-economic data such as population growth, income per capita, and even land tenure system for a deeper understanding of underlying conditions causing the landscape changes. Additionally, looking into the qualitative studies of management strategies and landscape planning and monitoring can give a clearer insight into the possible implementations to sustainable development. Community perceptions can also be assessed on the current land use strategies as the engagement of stakeholders is vital in formulating landscape strategies and policies to maintain the balance between urban development and environmental conservation. As the changes in the landscape are mainly due to infrastructure development, assessing the environmental impacts of these projects in relation to ecosystem integrity can give ways to strategize mitigation measures and minimization of urbanization effects. Lastly, designing and implementing restoration and rehabilitation projects for degraded landscapes can serve to enhance ecosystem resilience. This can be conducted either with the use of remote sensing techniques or ground-based monitoring. By means of addressing the complex factors driving the changes in vegetation and temperature

dynamics, policymakers can develop effective strategies for sustainable development and climate resilience in the province.

5. Acknowledgements

NHAD acknowledges the DOST- Philippine Council for Agriculture, Aquatic and Natural Resources Research and Development (PCAARRD) for the Balik Scientist grant. KJAR and JELD acknowledges Deutscher Akademischer Austauschdienst (DAAD) German Academic Exchange Service for the in Country/in Region Scholarship. PASM and AOP would like to thank the DOST – Accelerated Science and Technology Human Resource Development Program (ASTHRDP) for the Scholarship. The authors declare no conflicts of interest.

6. References

Almadrones-Reyes, K. J., & Dagamac, N. H. A. (2023). Land-use/land cover change and land surface temperature in Metropolitan Manila, Philippines using Landsat imagery. *GeoJournal*, *88*(2), 1415-1426. [Crossref]

Avdan, U., & Jovanovska, G. (2016). Algorithm for automated mapping of land surface temperature using LANDSAT 8 satellite data. *Journal of Sensors*, 1-8. [Crossref]

Bala, R., Prasad, R., Yadav, V. P., & Sharma, J. (2018). A comparative study of land surface temperature with different indices on heterogeneous land cover using Landsat 8 data. *The International Archives of the Photogrammetry, Remote Sensing and Spatial Information Sciences*, *42*, 389-394. [Crossref]

Barsi, J. A., Schott, J. R., Palluconi, F. D., Helder, D. L., Hook, S. J., Markham, B. L., Chander, G., & O'donnell, E. M. (2003). Landsat TM and ETM+ thermal band calibration. *Canadian Journal of Remote Sensing*, *29*(2), 141-153. [Crossref]

Buchori, I., Rahmayana, L., Pangi, P., Pramitasari, A., Sejati, A. W., Basuki, Y., & Bramiana, C. N. (2022). In situ urbanization-driven industrial activities: the Pringapus enclave on the rural-urban fringe of Semarang Metropolitan Region, Indonesia. *International Journal of Urban Sciences*, *26*(2), 244-267. [Crossref]

Chase, T. N., Pielke Sr, R. A., Kittel, T. G. F., Nemani, R. R., & Running, S. W. (2000). Simulated impacts of historical land cover changes on global climate in northern winter. *Climate Dynamics*, *16*, 93-105. [Crossref]

Chen, L., Li, M., Huang, F., & Xu, S. (2013). Relationships of LST to NDBI and NDVI in Wuhan City based on Landsat ETM+ image. In *2013 6th International Congress on Image and Signal Processing (CISP)*, (2), 840-845. IEEE

Dalling, J. W. (2008). Pioneer species. Encyclopedia of Ecology, 181–184.

Doygun, H., & Alphan, H. (2006). Monitoring urbanization of Iskenderun, Turkey, and its negative implications. *Environmental Monitoring and Assessment*, *114*, 145-155. [Crossref]

Ekwurzel, B., Boneham, J., Dalton, M. W., Heede, R., Mera, R. J., Allen, M. R., & Frumhoff, P. C. (2017). The rise in global atmospheric CO2, surface temperature, and sea level from emissions traced to major carbon producers. *Climatic Change*, *144*(4), 579-590. [Crossref]

Fang, J., Zhu, J., Wang, S., Yue, C., & Shen, H. (2011). Global warming, human-induced carbon emissions, and their uncertainties. *Science China Earth Sciences*, *54*, 1458-1468. [Crossref]

Gebre, S. L., Cattrysse, D., Alemayehu, E., & Van Orshoven, J. (2021). Multi-criteria decision making methods to address rural land allocation problems: A systematic review. *International Soil and Water Conservation Research*, *9*(4), 490–501. [Crossref]

Gaur, A., Eichenbaum, M. K., & Simonovic, S. P. (2018). Analysis and modelling of surface Urban Heat Island in 20 Canadian cities under climate and land-cover change. *Journal of environmental management*, *206*, 145-157. [Crossref]

Guha, S., Govil, H., & Mukherjee, S. (2017). Dynamic analysis and ecological evaluation of urban heat islands in Raipur city, India. *Journal of Applied Remote Sensing*, *11* (3), 036020-036020. [Crossref]

He, J. F., Liu, J. Y., Zhuang, D. F., Zhang, W., & Liu, M. L. (2007). Assessing the effect of land use/land cover change on the change of urban heat island intensity. *Theoretical and applied climatology*, *90*, 217-226. [Crossref]

Hilario, F., de Guzman, R., Ortega, D., Hayman, P., & Alexander, B. (2009). El Niño Southern Oscillation in the Philippines: impacts, forecasts, and risk management. *Philippine Journal of Development*, *36*(1), 9.

Jiménez-Muñoz, J. C., Sobrino, J. A., Gillespie, A., Sabol, D., & Gustafson, W. T. (2006). Improved land surface emissivities over agricultural areas using ASTER NDVI. *Remote Sensing of Environment*, *103*(4), 474-487. [Crossref]

Kasperson, J. X., Kasperson, R. E., & Turner, B. L. (1995). Regions at risk: Comparisons of threatened environments. United Nations Univ. Press, Tokyo.

Khandelwal, S., Goyal, R., Kaul, N., & Mathew, A. (2018). Assessment of land surface temperature variation due to change in elevation of area surrounding Jaipur, India. *The Egyptian Journal of Remote Sensing and Space Science*, *21*(1), 87-94. [Crossref]

Kumar, K. S., Bhaskar, P. U., & Padmakumari, K. (2012). Estimation of land surface temperature to study urban heat island effect using Landsat ETM+ image. *International Journal of Engineering Science and Technology*, *4*(2), 771-778.

LaGro, J. A. (2005). Land-use classification. *Encyclopedia of Soils in the Environment*, *7*(3), 321-328.

Lasco, R. D., Pulhin, F. B., & Banaticla, M. R. N. (2005). Potential carbon sequestration projects in the Philippines. Environmental Forestry Program. *University of the Philippines Los Banos, College of Forestry and Natural Resources, College, Laguna*.

Limbo-Dizon, J. E., & Dagamac, N. H. A. (2023). Assessment of coastal change detection on an urban coastline: A case study in metropolitan Manila, Philippines. In *IOP Conference Series: Earth and Environmental Science*, *1165*(1), 12-15. IOP Publishing.

Malik, M. S., Shukla, J. P., & Mishra, S. (2019). Relationship of LST, NDBI and NDVI using Landsat-8 data in Kandaihimmat watershed, Hoshangabad, India.

Maruna, M., Crnčević, T., & Milojević, M. P. (2019). The institutional structure of land use planning for urban forest protection in the post-socialist transition environment: Serbian experiences. *Forests*, *10*(7), 560. [Crossref]

Meeus, S. J., & Gulinck, H. (2008). Semi-urban areas in landscape research: a review. *Living Reviews in Landscape Research*, *2*. [Crossref]

Morris, K. I., Chan, A., Morris, K. J. K., Ooi, M. C. G., Oozeer, M. Y., Abakr, Y. A., Nadzir, M. S. M., Mohammed, I. Y., & Al-Qrimli, H. F. (2017). Impact of urbanization level on the interactions of urban area, the urban climate, and human thermal comfort. *Applied Geography*, *79*, 50-72. [Crossref]

Murdiyarso, D., & Skutsch, M. (Eds.). (2006). Community forest management as a carbon mitigation option: case studies. CIF

Naikoo, M. W., Islam, A. R. M. T., Mallick, J., & Rahman, A. (2022). Land use/land cover change and its impact on surface urban heat island and urban thermal comfort in a metropolitan city. *Urban Climate*, *41*, 101052. [Crossref]

Nazeer, M., Nichol, J. E., & Yung, Y. K. (2014). Evaluation of atmospheric correction models and Landsat surface reflectance product in an urban coastal environment. *International journal of remote sensing*, *35*(16), 6271-6291. [Crossref]

Nowak, D. J., Rowntree, R. A., McPherson, E. G., Sisinni, S. M., Kerkmann, E. R., & Stevens, J. C. (1996). Measuring and analyzing urban tree cover. *Landscape and Urban Planning*, *36*(1), 49–57. [Crossref]

Peng, S-S., Piao, S., Zeng, Z., Ciais, P., Zhou, L., Li, L. Z. X., Myneni, R. B., Yin, Y., & Zeng, H. (2014). Afforestation in China cools local land surface temperature. *Proceedings of the National Academy of Sciences*, *111*(8), 2915-2919. [Crossref]

Peng, X., Wu, W., Zheng, Y., Sun, J., Hu, T., & Wang, P. (2020). Correlation analysis of land surface temperature and topographic elements in Hangzhou, China. *Scientific Reports*, *10*(1), 10451. [Crossref]

Phelan, K., Hurley, J., & Bush, J. (2018). Land-use planning's role in Urban Forest Strategies: Recent local government approaches in Australia. *Urban Policy and Research*, *37*(2), 215–226. [Crossref]

Poursanidis, D., Chrysoulakis, N., & Mitraka, Z. (2015). Landsat 8 vs. Landsat 5: A comparison based on urban and peri-urban land cover mapping. *International Journal of Applied Earth Observation and Geoinformation*, *35*, 259-269. [Crossref]

Qin, Z., Karnieli, A., & Berliner, P. (2001). A mono-window algorithm for retrieving land surface temperature from Landsat TM data and its application to the Israel-Egypt border region. *International Journal of Remote Sensing*, *22*(18), 3719-3746. [Crossref]

Ramachandra, T. V., Bharath, A. H., & Sowmyashree, M. V. (2015). Monitoring urbanization and its implications in a mega city from space: Spatiotemporal patterns and its indicators. *Journal of Environmental Management*, *148*, 67-81. [Crossref]

Regmi, R. K. (2017). Urbanization and related environmental issues of Metro Manila. *Journal of Advanced College of Engineering and Management*, *3*, 79-92. [Crossref]

Saha, S., Saha, A., Das, M., Sarkar, R., & Das, A. (2021). Analyzing spatial relationship between land use/land cover (LULC) and land surface temperature (LST) of three urban agglomerations (UAs) of Eastern India. *Remote Sensing Applications: Society and Environment*, *22*, 100507. [Crossref]

Schneider, K., & Mauser, W. (1996). Processing and accuracy of Landsat Thematic Mapper data for lake surface temperature measurement. *International Journal of Remote Sensing*, *17*(11), 2027-2041. [Crossref]

Sobrino, J. A., & Raissouni, N. (2000). Toward remote sensing methods for land cover dynamic monitoring: Application to Morocco. *International Journal of Remote Sensing*, *21*(2), 353-366. [Crossref]

Stathopoulou, M., & Cartalis, C. (2007). Daytime urban heat islands from Landsat ETM+ and Corine land cover data: An application to major cities in Greece. *Solar Energy*, *81*(3), 358-368. [Crossref]

Stempihar, J. J., Pourshams-Manzouri, T., Kaloush, K. E., & Rodezno, M. C. (2012). Porous asphalt pavement temperature effects for urban heat island analysis. *Transportation Research Record*, *2293*(1), 123-130. [Crossref]

Sun, F., Liu, M., Wang, Y., Wang, H., & Che, Y. (2020). The effects of 3D architectural patterns on the urban surface temperature at a neighborhood scale: Relative contributions and marginal effects. *Journal of Cleaner Production*, *258*, 120706. [Crossref]

Tejada, S. Q., Tuddao Jr, V. B., Juanillo, E., & Brampio, E. (2014). Drought conditions and management strategies in the Philippines. *Country Report*, 2-5.

Tiangco, M., Lagmay, A. M. F., & Argete, J. (2008). ASTER-based study of the night-time urban heat island effect in Metro Manila. *International Journal of Remote Sensing*, *29*(10), 2799-2818. [Crossref]

Tinoy, M. M., Novero, A. U., Landicho, K. P., Baloloy, A. B., & Blanco, A. C. (2019). Urban effects on land surface temperature in Davao City, Philippines. *The International Archives of the Photogrammetry, Remote Sensing and Spatial Information Sciences*, *42*, 433-440. [Crossref]

Tran, D. X., Pla, F., Latorre-Carmona, P., Myint, S. W., Caetano, M., & Kieu, H. V. (2017). Characterizing the relationship between land use land cover change and land surface temperature. *ISPRS Journal of Photogrammetry and Remote Sensing*, *124*, 119-132. [Crossref]

Uddin, A. S. M. S., Khan, N., Islam, A. R. M. T., Kamruzzaman, M., & Shahid, S. (2022). Changes in urbanization and urban heat island effect in Dhaka city. *Theoretical and Applied Climatology*, *147*(3-4), 891-907. [Crossref]

United Nations. (2015). General Assembly Resolution A/RES/70/1. Transforming Our World, the 2030 Agenda for Sustainable Development.

United Nations Framework Convention on Climate Change (UNFCCC). Paris Agreement. 2015. Available online: https://unfccc.int/sites/default/files/english_paris_agreement.pdf.

United Nations Human Settlements Programme (UN HABITAT). New Urban Agenda. A/RES/71/256. United Nations, 2017. Available online: http://habitat3.org/wp-content/uploads/NUA-English.pdf

Verheye, W. H. (1997). Land use planning and national soils policies. *Agricultural Systems*, *53*(2-3), 161-174. [Crossref]

Vitousek, P. M., Mooney, H. A., Lubchenco, J., & Melillo, J. M. (1997). Human domination of Earth's ecosystems. *Science*, *277*(5325), 494-499.

Wang, F., Qin, Z., Song, C., Tu, L., Karnieli, A., & Zhao, S. (2015). An improved mono-window algorithm for land surface temperature retrieval from Landsat 8 thermal infrared sensor data. *Remote sensing*, *7*(4), 4268-4289. [Crossref]

Yang, L., Qian, F., Song, D-X., & Zheng, K-J. (2016). Research on urban heat-island effect. *Procedia Engineering*, *169*, 11-18. [Crossref]

Yuan, F., & Bauer, M. E. (2007). Comparison of impervious surface area and normalized difference vegetation index as indicators of surface urban heat island effects in Landsat imagery. *Remote Sensing of Environment*, *106*(3), 375-386. [Crossref]

Zhou, W., Huang, G., & Cadenasso, M. L. (2011). Does spatial configuration matter? Understanding the effects of land cover pattern on land surface temperature in urban landscapes. *Landscape and urban planning*, *102*(1), 54-63. [Crossref]

Zhou, W., Qian, Y., Li, X., Li, W., & Han, L. (2014). Relationships between land cover and the surface urban heat island: seasonal variability and effects of spatial and thematic resolution of land cover data on predicting land surface temperatures. *Landscape Ecology*, *29*, 153-167. [Crossref]

Zhou, X., & Chen, H. (2018). Impact of urbanization-related land use land cover changes and urban morphology changes on the urban heat island phenomenon. *Science of the Total Environment*, *635*, 1467-1476. [Crossref]